

Supporting Information

A Step Toward an NIR-Emitting ESIPT Probe For Smart Zn²⁺ Sensing In Different Environments

Junfeng Wang,^{1,2} Yingbo Li,³ Yi Pang*¹

¹ Department of Chemistry & Maurice Morton Institute of Polymer Science, The University of Akron, Ohio 44325, USA

² Gordon Center for Medical Imaging, Massachusetts General Hospital and Harvard Medical School, 125 Nashua Street, Suite 660, Boston, Massachusetts 02114, United States.

³ State Key Laboratory of Natural and Biomimetic Drugs, School of Pharmaceutical Sciences, Peking University, Beijing 100191, China

*Correspondence to Dr. Yi Pang (yp5@uakron.edu)

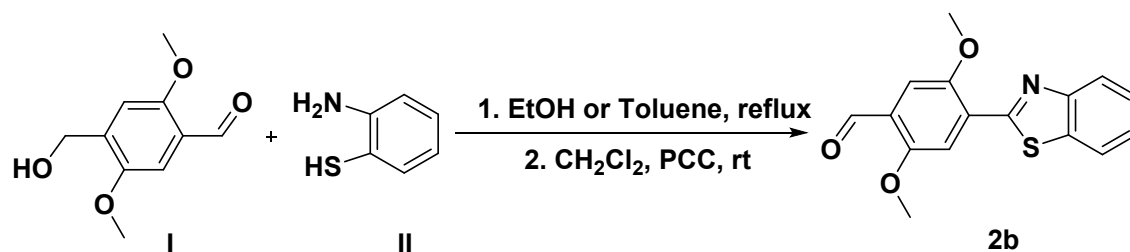
General experimental procedures for synthesis and characterization

Instrumentation. UV-Visible spectroscopy data were acquired with Hewlett Packard-8453 diode array spectrophotometer, and fluorescence spectroscopy data were acquired with HORIBA Fluoromax-4 spectrofluorometer at room temperature. ^1H NMR and ^{13}C NMR spectra were obtained on a Varian 500 MHz spectrometers respectively in deuterated chloroform (CDCl_3) at room temperature.

Synthesis. All solvents and reagents for chemical synthesis and spectroscopic evaluations were purchased from Acros Organics and Fisher scientific and they were used as received without further purification unless specified otherwise.

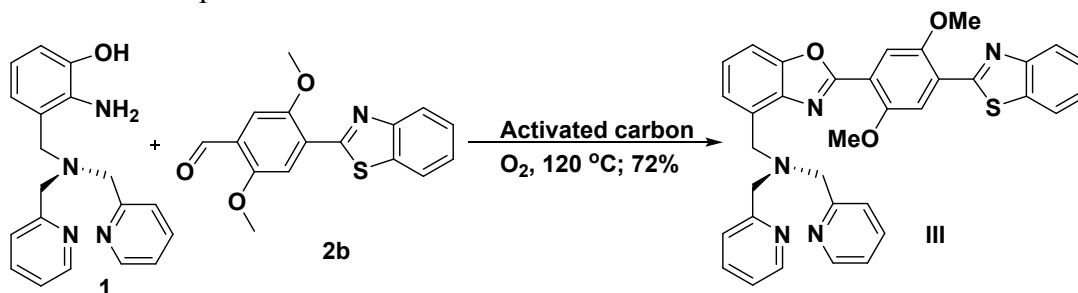
General Procedure for spectroscopic titration. Spectroscopic grade solvents were used for spectroscopic analysis of the probes. The stock solutions of Zinhbo-9 (10 mM in DMSO) and $\text{Zn}(\text{OAc})_2$ (1 mM in DMSO) were prepared in advance and stored at $0\text{ }^\circ\text{C}$. During the titration, the Zinhbo-9 solution in CH_2Cl_2 (10 μM) was freshly prepared by adding 2 μL of Zinhbo-9 stock solution (10 mM in DMSO) into a quartz cell containing 2 mL of CH_2Cl_2 . The titration was then carried out by adding $\text{Zn}(\text{OAc})_2$ (1 mM in DMSO) in 2 μL increment. Spectroscopic data were analyzed and processed by using Origin® Lab software.

Synthesis of 2b



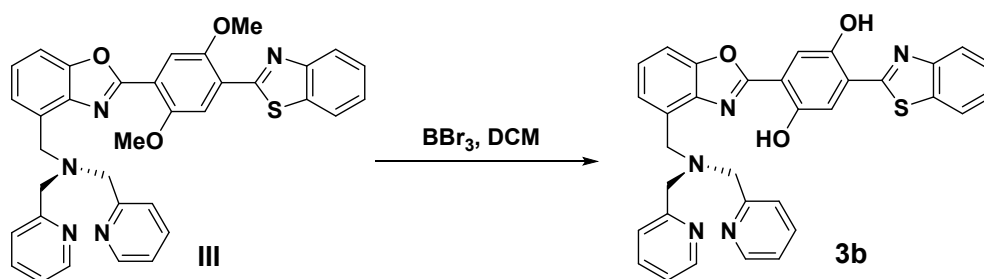
Compound **2b** was synthesized by the modified procedure based on our previous reported method (*RSC Advances*, **2013**, 3, 10208). Intermediates **I** (590 mg) and **II** (380 mg) were dissolved in EtOH or toluene (50 mL), and the mixture was refluxed overnight. The resulting mixture was concentrated under vacuum and dried in a vacuum oven overnight. The crude product was then re-dissolved in 80 mL anhydrous DCM without purification, then DDQ (600 mg) was added in the solution and the mixture was stirred at room temperature overnight, followed by addition of PCC (1.0 g) and silica gel (4.0 g) at room temperature. The reaction mixture was further stirred at room temperature for another 10 hours. Finally, the mixture was stirred overnight and then filtered through a short pad of silica and washed by EtOAc. The organic phase was collected, concentrated in vacuum, and purified on a silica gel column to give **2b** in 67 % yield as yellow solid. ¹H NMR (300 MHz, CDCl₃): 10.52 (1H, s), 8.27 (1H, s), 8.13 (1H, d, *J* = 8.4 Hz), 7.96 (1H, d, *J* = 8.4 Hz), 7.53 (1H, tri, *J* = 7.5 Hz) overlapped with 7.53 (1H, s), 4.01 (6H, s). ¹³C NMR (75 MHz, CDCl₃): 189.1, 161.4, 156.1, 152.0, 151.3, 136.7, 128.6, 126.2, 126.1, 125.3, 123.2, 121.4, 112.5, 110.5, 56.3, 56.3. TOS-ESI-MS⁺ (*m/z*): calcd for C₁₆H₁₄NO₃S, [M + H]⁺, 300.0694, found, 300.1095.

Synthesis of Compound III



Intermediate **1** (600 mg) and **2b** (800 mg) were dissolved in DMF (1.0 mL), which was subsequently diluted by xylenes to 30 mL. After addition of activated carbon (400 mg), the resulting black mixture was well stirred at 110-120 °C, and the oxygen gas was bubbled into the reaction mixture. Upon completion of the reaction, the mixture was filtered and washed by EtOH. The resulting crude product was concentrated and purified on a silica gel column to give **III** in a 72% yield as a brown solid. ¹H NMR (300 MHz, CDCl₃): 8.52 (2H, d, *J* = 4.8 Hz), 8.33 (1H, s), 8.13 (1H, d, *J* = 8.1 Hz), 7.96 (1H, d, *J* = 7.8 Hz), 7.91 (1H, s), 7.79 (2H, d, *J* = 8.1 Hz), 7.65 (2H, td, *J* = 1.5 Hz, *J* = 7.5 Hz), 7.58 (1H, d, *J* = 7.5 Hz), 7.55-7.50 (2H, m), 7.41 (1H, t, *J* = 7.8 Hz), 7.36 (1H, t, *J* = 7.8 Hz), 7.15-7.13 (2H, m), 4.26 (2H, s), 4.16 (3H, s), 4.14 (3H, s), 3.96 (4H, s); ¹³C NMR (75 MHz, CDCl₃): 161.8, 160.7, 160.1, 152.8, 152.1, 151.3, 150.7, 149.0, 141.2, 136.5, 136.4, 131.4, 126.160.3, 57.0, 56.6, 53.5. TOS-ESI-MS⁺ (*m/z*): calcd for C₃₅H₃₀N₅O₃S, [M + H]⁺, 600.2069, found, 600.1042.

Synthesis of **3b**



Compound **3b** was synthesized by using the reported method (see ref: *RSC Advances*, **2013**, 3, 10208): Compound **III** (200 mg) was dissolved in anhydrous DCM, and the solution was cooled to -78 °C. Then BBr₃ (300 mg) was added slowly, and the resulting mixture was warmed to room temperature and stirred overnight. The reaction mixture was quenched by addition of water, and DCM layer was separated on a silica gel column in 70% yield as a yellow solid. ¹H NMR (300 MHz, CDCl₃): δ 12.01 (1H, s), 10.95 (1H, s), 8.54 (2H, d, *J* = 4.5 Hz), 7.99 (1H, d, *J* = 7.8 Hz), 7.91 (1H, d, *J* = 7.2 Hz), 7.72 (1H, s), 7.69 (2H, dd, *J* = 1.5 Hz, *J* = 7.2 Hz), 7.64 (2H, d, *J* = 7.5 Hz), 7.53-7.44 (3H, m), 7.45 (1H, s), 7.43 (1H, d, *J* = 8.7 Hz), 7.34 (1H, d, *J* = 7.8 Hz), 7.15 (2H, td, *J* = 1.5 Hz, *J* = 5.1 Hz), 4.13 (2H, s), 3.91 (4H, s). ¹³C NMR (75 MHz, CDCl₃): δ 168.0, 161.5, 159.5, 151.9, 150.9, 150.5, 149.2, 149.0, 139.4, 136.6, 133.1, 130.4, 126.9, 126.1, 126.0, 125.7, 122.8, 122.5, 122.0, 121.6,

120.7, 115.6, 115.0, 114.0, 109.5, 60.3, 53.6. TOS-ESI-MS⁺ (m/z): calcd for C₃₃H₂₆N₅O₃S, [M + H⁺]⁺, 572.1756, found, 572.1738. Its zinc complex: calcd for C₃₃H₂₅N₅O₃SZn, [M + Zn²⁺ - H⁺]⁺, 634.0891, found, 634.0919.

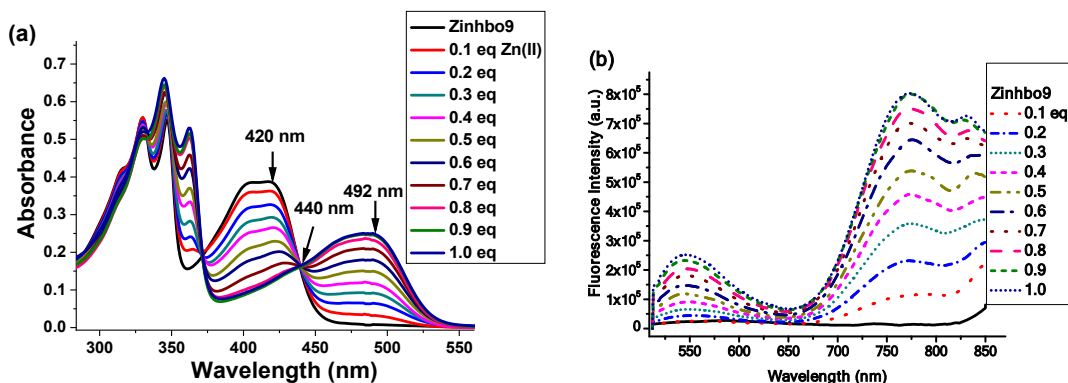


Fig. S1 UV-vis (a) and fluorescent spectra (b) of **Zinhbo-9** (10 μ M) in CH₂Cl₂ upon addition of different equivalent of Zn²⁺. (b) The samples were excited at 492 nm.

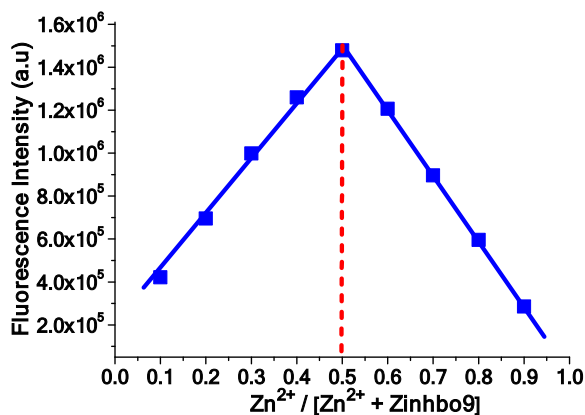


Fig. S2 The Job's plot of **Zinhbo9** in HEPES buffer (10 mM, pH = 7.4) containing 50% EtOH: the fluorescence was monitored at 542 nm and the total concentration of [Zn²⁺] + [Zinhbo9] = 1 μ M.

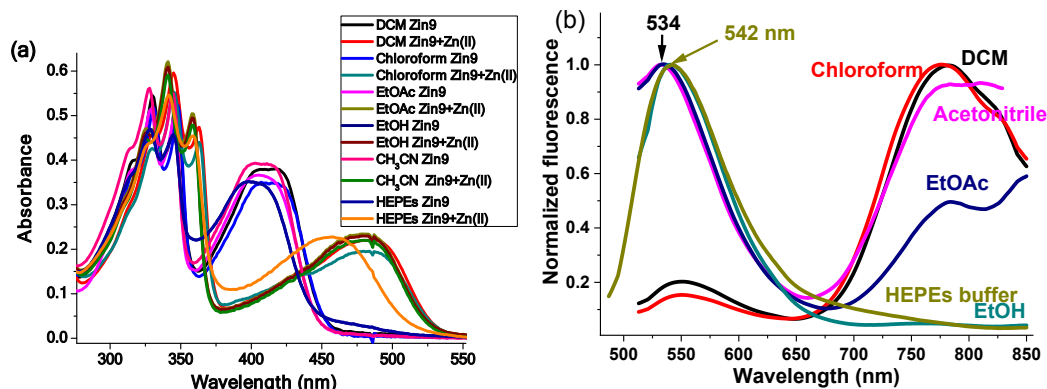


Figure S3. (a) UV-vis spectra of **Zinhbo-9** in different solvents before (broken line) and after addition of 5.0 equivalent of Zn^{2+} (solid line). (b) normalized fluorescent spectra after addition of Zn^{2+} , while the samples were excited at λ_{max} .

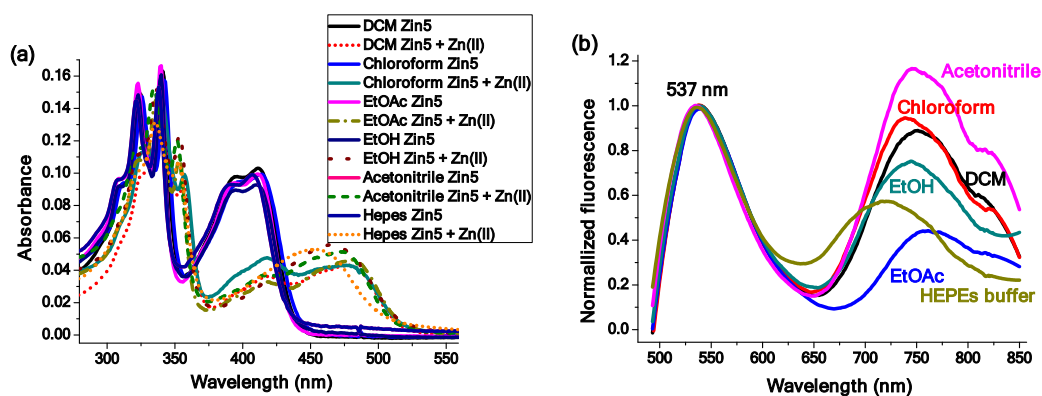


Fig. S4 UV-vis (a) and normalized fluorescent spectra (b) of **Zinhbo-5** in different solvents upon addition of 5.0 equivalent of Zn^{2+} . (b) The samples were excited at λ_{max} .

Table S1 Basic properties of **Zinhbo5-Zn** and **Zinhbo9-Zn** in different solvents.

Zin5+Zn²⁺	λ_{ab} (nm)	λ_{em} (nm)	<i>enol:keto</i>	Zin9+Zn²⁺	λ_{ab} (nm)	λ_{em} (nm)	<i>enol:keto</i>
DCM	480	537; 752	1:0.88	DCM		534; 777	0.2
CHCl ₃	480	537; 742	1:0.94	CHCl ₃		534; 775	0.15
CH ₃ CN	475	537; 747	1:1.17	CH ₃ CN		534; 777	1.08
EtOAc	482	537; 757	1:0.44	EtOAc		534; 782	2
EtOH	472	537; 742	1:0.75	EtOH		542; -	very large
Buffer	457	537; 722	1:0.58	Buffer		542; -	very large

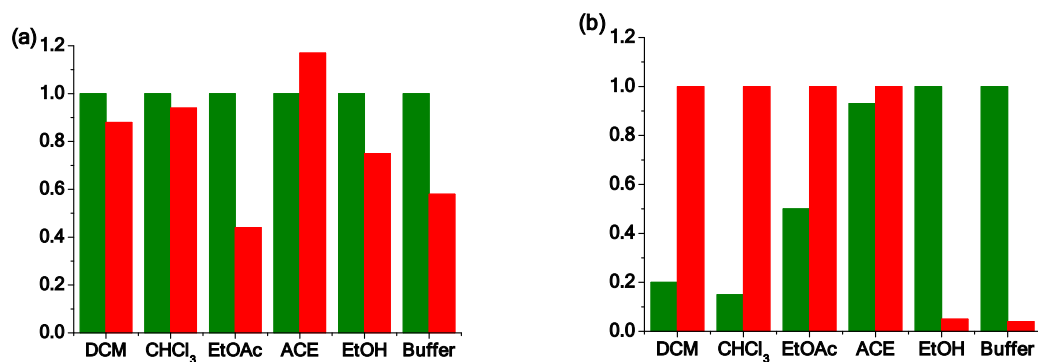


Fig. S5 The ratio of fluorescence intensity plot towards *enol* emission (green bars) and *keto* emission (red bars) of **zinhbo5** (a) and **zinhbo9** (b) upon addition of 5.0 equivalent Zn^{2+} in different solvents.

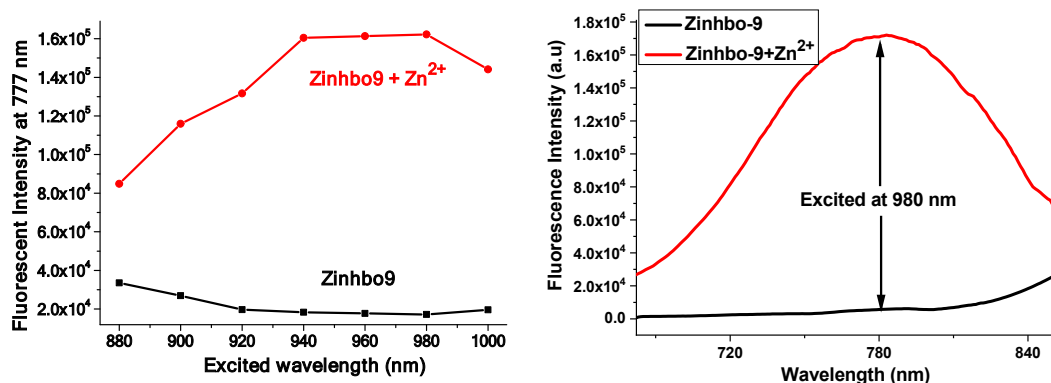


Fig. S6 Left panel: Fluorescent excitation spectra of **Zinhbo-9** and **Zinhbo-9-Zn** when emission was monitored at 777 nm in DCM (excitation wavelengths from 880-1000 nm). The plot showed that the zinc selective sensor was excitable near 940-1000 nm (slit = 5 nm) via two photon absorption. Right panel: Fluorescence spectra of **Zinhbo-9** upon addition of 1.0 equivalent of Zn^{2+} in DCM when being excited at 980 nm.

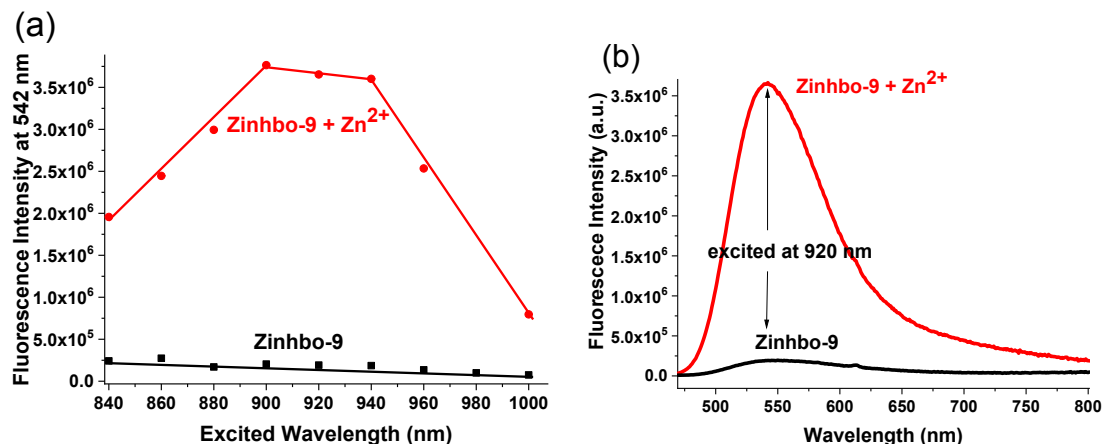


Fig. S7 (a) Fluorescent response of **Zinhbo-9** and **Zinhbo-9-Zn** at 542 nm in HEPEs buffer (10 mM, pH = 7.4) containing 50% EtOH when being excited at different wavelengths (from 880-1000 nm, slit 5 nm). The plot revealed that the zinc selective sensor was excitable near 880-960 nm via two photon absorption. (b) Fluorescence spectra of **Zinhbo-9** (10 μ M) upon addition of 1.0 equivalent of Zn^{2+} in HEPEs buffer (10 mM, pH = 7.4) containing 50% EtOH when being excited at 920 nm.

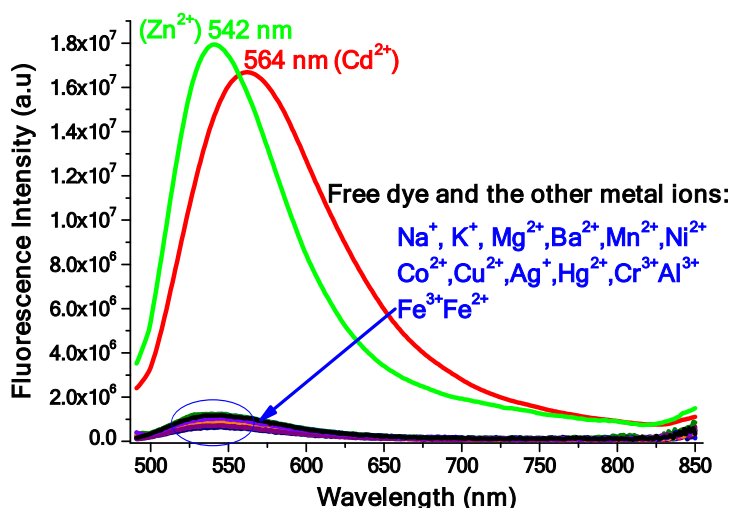


Fig. S8 Fluorescent spectra of **Zinhbo-9** (10 μ M) upon addition of 5.0 equivalent of different metal ions in HEPEs buffer (10 mM, pH = 7.4) containing 50% EtOH. The sensor only showed fluorescent turn-on towards Zn^{2+} and Cd^{2+} .

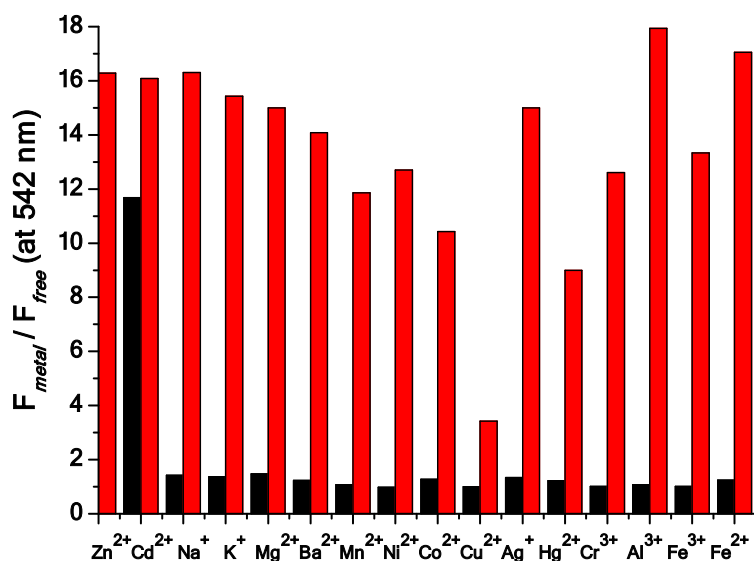


Fig S9. Relative fluorescence ratio (I_{542}/I_{627}) of **Zinhbo-9** (10 μM) upon addition of 5.0 equiv. of different metal ions (black bars), followed by addition of 5.0 equivalent of Zn^{2+} (red bars) in HEPEs buffer (10 mM, pH = 7.4) containing 50% EtOH.

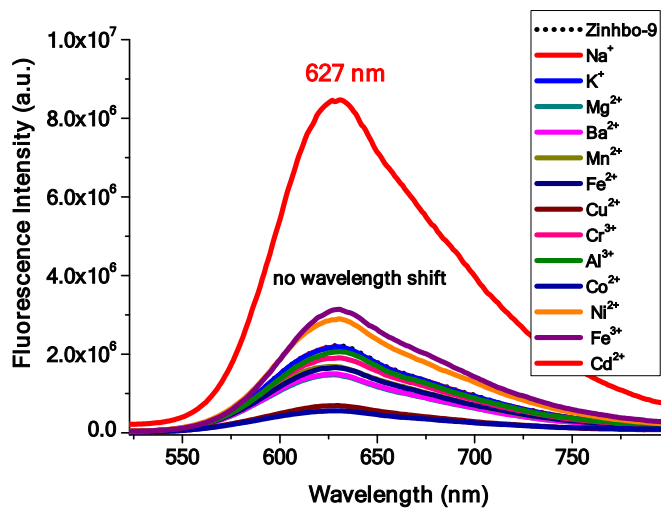


Fig S10. Fluorescence spectra of **Zinhbo-9** (10 μM) in CH_2Cl_2 upon addition of 2.0 equivalents of metal ions; none of them induced NIR fluorescent turn-on and did not induce much fluorescent change. And only Cu^{2+} and Co^{2+} induced slight fluorescent quenching.

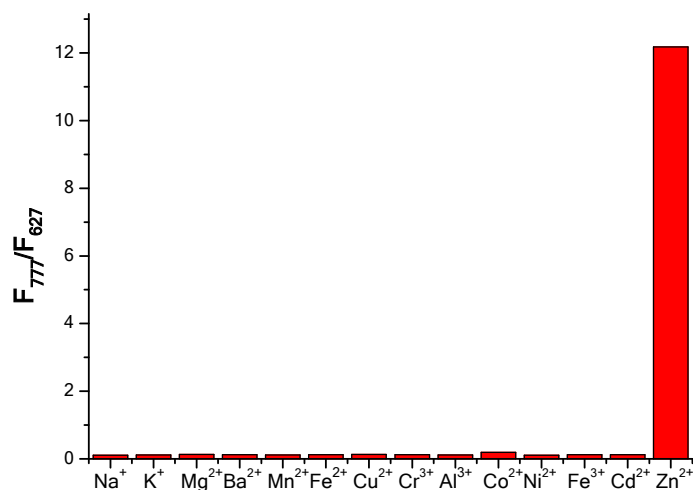


Fig S11. Relative fluorescence ratio (I_{777}/I_{627}) of **Zinhbo-9** (10 μM) in CH_2Cl_2 upon addition of 2.0 equiv. of different metal ions, which reveals that only zinc ion could induce NIR fluorescent turn-on.

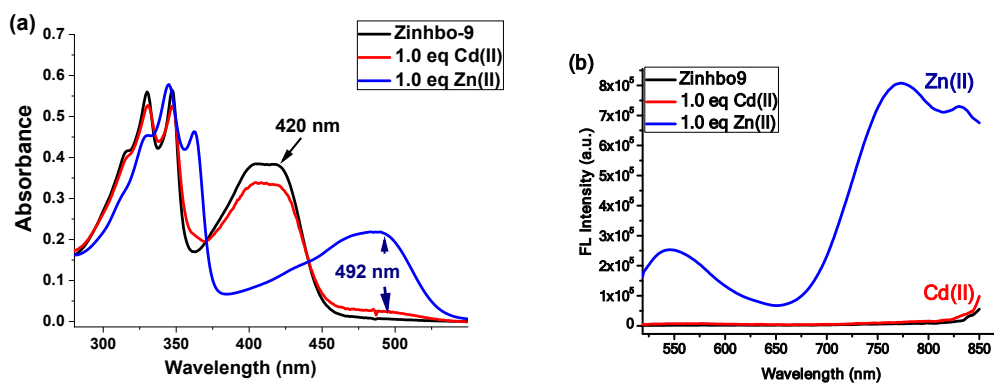


Fig. S12 Comparison of UV-vis (a) and fluorescent spectra (b) of **Zinhbo-9** (10 μM) in DCM upon addition of 1.0 equivalent of Cd^{2+} and Zn^{2+} . The samples were excited at 492 nm. Cadmium binding to **Zinhbo-9** did not induce UV-vis change at 492 nm, and almost no NIR emission was detected after addition of Cd^{2+} , which could easily distinguish Zn^{2+} from Cd^{2+} .

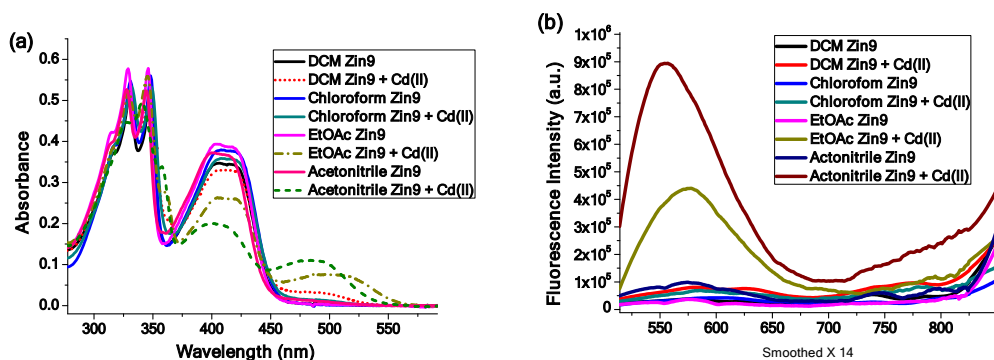


Fig. S13. UV-vis (a) and fluorescent spectra (b) of **Zinhbo-9** (10 μM) in different solvents upon addition of 1.0 equivalent of Cd²⁺. **Zinhbo-9** did not show NIR turn-on response towards Cd²⁺ in all the solvents tested.

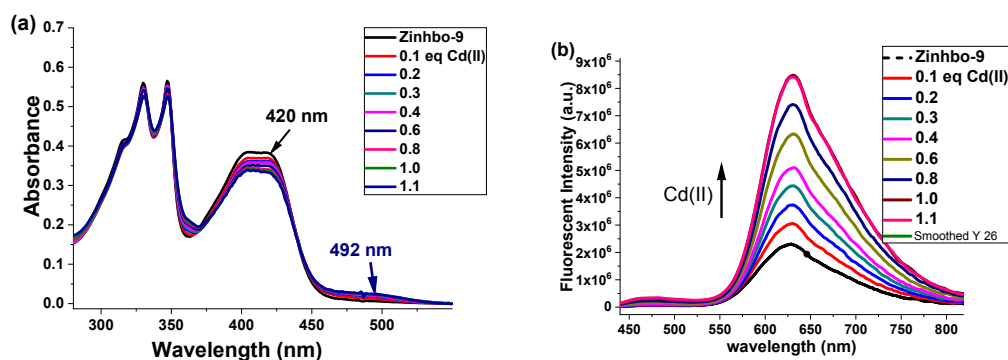


Fig. S14. UV-vis (a) and fluorescent spectra (b) of **Zinhbo-9** (10 μM) in DCM upon addition of different equivalent of Cd²⁺. The fluorescence spectra were obtained by excitation at 420 nm.

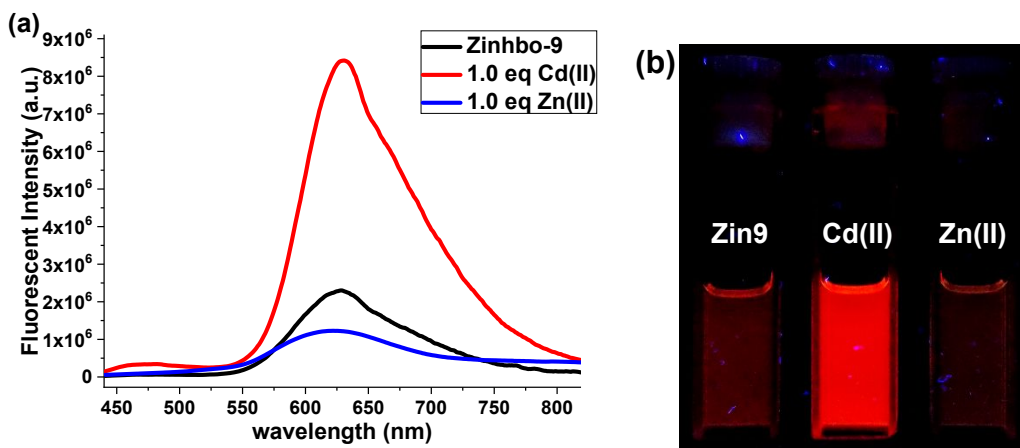


Fig. S15 (a) Fluorescent spectra of **Zinhbo-9** (10 μM) in DCM upon addition of 1.0 equivalent of Cd²⁺ and Zn²⁺ respectively. The samples were excited at 420 nm when acquiring the fluorescence spectra. (b) The images of **Zinhbo-9** (10 μM) in DCM upon addition of 1.0 equivalent of Cd²⁺ and Zn²⁺, when the sample solutions were excited with a 365nm UV lamp.

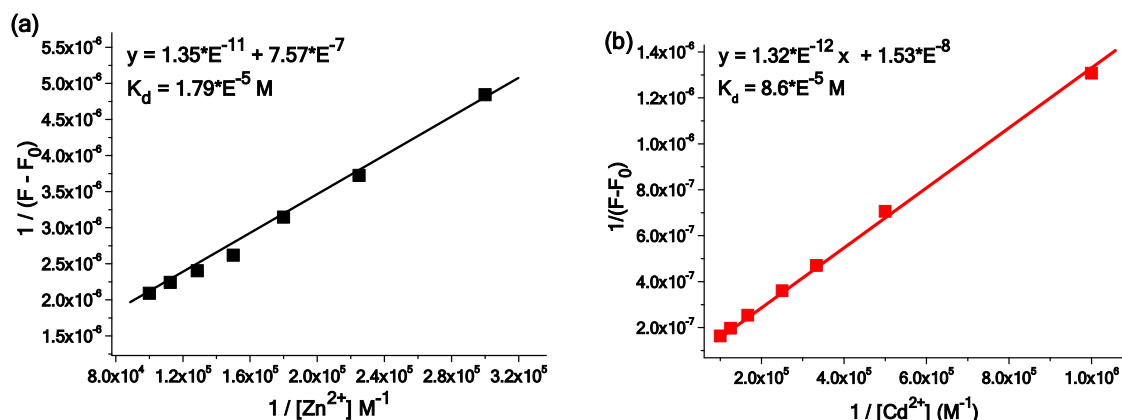


Fig. S16 Benesi-Hildebrand plot of **Zinhbo-9** with Zn^{2+} (a) and Cd^{2+} (b) in DCM. The disassociation constants were calculated as $17.9 \mu M$ for Zn^{2+} and $86.0 \mu M$ for Cd^{2+} binding with **Zinhbo-9** respectively. This reveals that Zn^{2+} binds to **Zinhbo-9** stronger than Cd^{2+} in DCM (about 5 times stronger).

The plot was constructed by using the fluorescence response at 630 nm for Cd^{2+} (Figure S14) and at 770 nm for Zn^{2+} (Figure S1), and by using the following equation:

$$\frac{1}{F - F_0} = \frac{1}{(F_{max} - F_0) \cdot [M]} \cdot \frac{1}{K_a} + \frac{1}{(F_{max} - F_0)}$$

$$= \frac{1}{(F_{max} - F_0) \cdot [M]} \cdot K_d + \frac{1}{(F_{max} - F_0)}$$

where F_0 is the fluorescence of ligand before addition of metal cation (Zn^{2+} or Cd^{2+}), and F_{max} is the fluorescence when all the ligand form the complex with the metal cation. The apparent binding constant K_a is calculated from the slope.

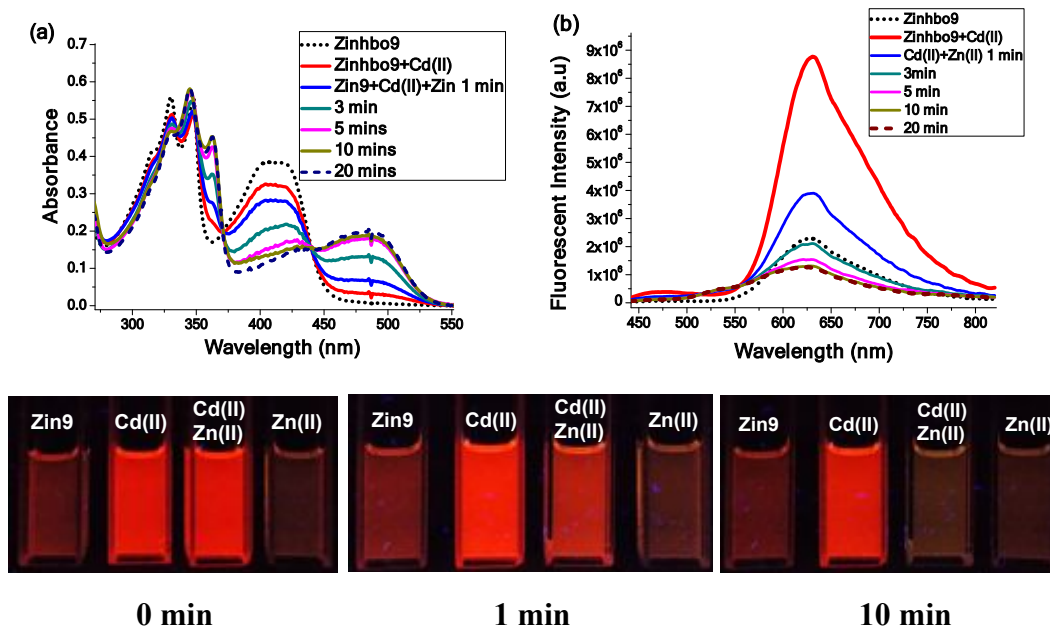


Fig. S17 Replacement of Cd^{2+} by Zn^{2+} in DCM was observed in DCM. Immediate replacement of Cd^{2+} by Zn^{2+} in DCM was observed (within 1 min). From the UV-vis (a) and fluorescent spectra (b) excited at 420 nm, we can see the total replacement was accomplished in about 10 mins. The result was consistent with the finding that **Zinhbo-9** exhibited stronger binding to Zn^{2+} than Cd^{2+} cation (Fig. S16).

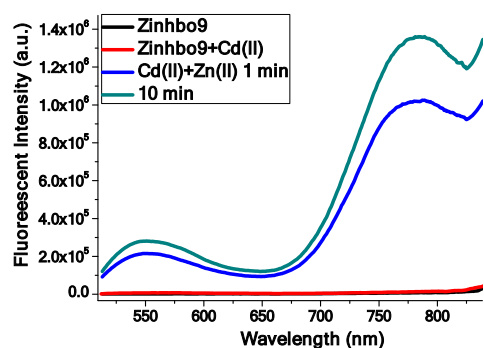


Fig. S18 Fluorescence spectra of **Zinhbo9** (10 μM) in DCM, followed by subsequent addition of Cd^{2+} (1 equiv), and Zn^{2+} (1 equiv). Replacement of Cd^{2+} by Zn^{2+} in DCM was clearly observable and immediate NIR fluorescence turn-on was detected (within 1 min) when excited at 492 nm, which easily identified Zn^{2+} from Cd^{2+} .

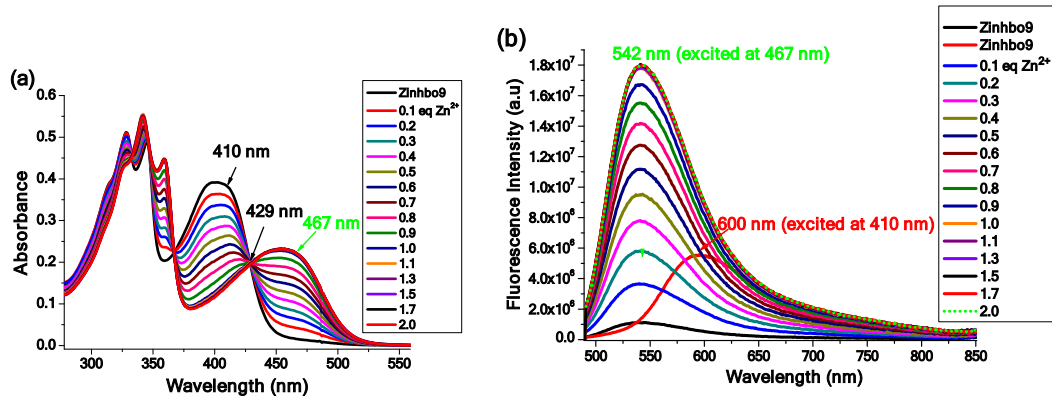


Fig. S19 UV-vis (a) and fluorescent spectra (b) change of **Zinhbo-9** (10 μ M) upon addition of different equivalent of Zn²⁺ in HEPES buffer (10 mM, pH = 7.4) containing 50% EtOH.

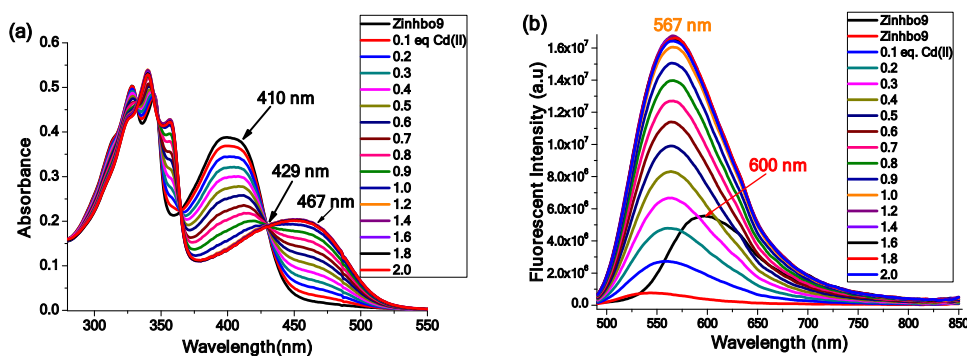


Fig. S20 UV-vis (a) and fluorescent spectra (b) change of **Zinhbo-9** (10 μ M) upon addition of different equivalent of Cd²⁺ in HEPES buffer (10 mM, pH = 7.4) containing 50% EtOH.

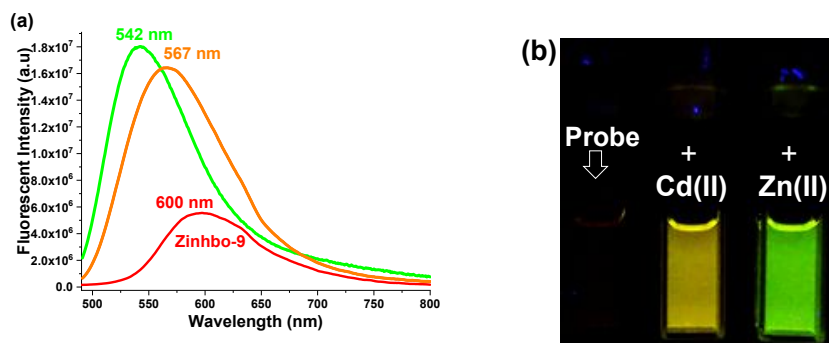


Fig. S21 (a) Fluorescent spectra of **Zinhbo-9** (10 μ M) in HEPES buffer (pH = 7.4) containing 50% EtOH upon addition of 5.0 equivalent of Cd²⁺ and Zn²⁺ respectively. The samples were excited at 467 nm. (b) The images of **Zinhbo-9** probe (10 μ M) in HEPES buffer (pH = 7.4) containing 50% EtOH upon addition of 5.0 equivalent of Cd²⁺ and Zn²⁺ captured under a 365nm UV lamp.

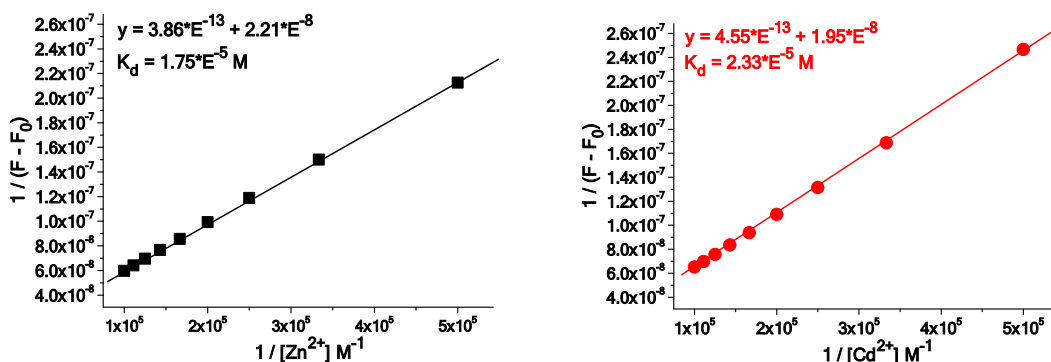


Fig. S22 Benesi-Hildebrand plot of **Zinhbo-9** with Zn^{2+} and Cd^{2+} in HEPES buffer (pH = 7.4) containing 50% EtOH. The disassociation constants were calculated as 17.5 μM for Zn^{2+} and 23.3 μM for Cd^{2+} binding with **Zinhbo-9** respectively, which reveals that Zn^{2+} binds to **Zinhbo-9** a little stronger than Cd^{2+} by about 1.33 times.

The plot was constructed by using the fluorescence response at 542 nm for Zn^{2+} (Figure S19) and at 567 nm for Cd^{2+} (Figure S20) and, by using the following equation:

$$\frac{1}{F - F_0} = \frac{1}{(F_{max} - F_0) \cdot [M]} \cdot \frac{1}{K_a} + \frac{1}{(F_{max} - F_0)}$$

$$= \frac{1}{(F_{max} - F_0) \cdot [M]} \cdot K_d + \frac{1}{(F_{max} - F_0)}$$

where F_0 is the fluorescence of ligand before addition of metal cation (Zn^{2+} or Cd^{2+}), and F_{max} is the fluorescence when all the ligand form the complex with the metal cation. K_a is association constant for the metal complex. The apparent binding constant K_a is calculated from the slope.

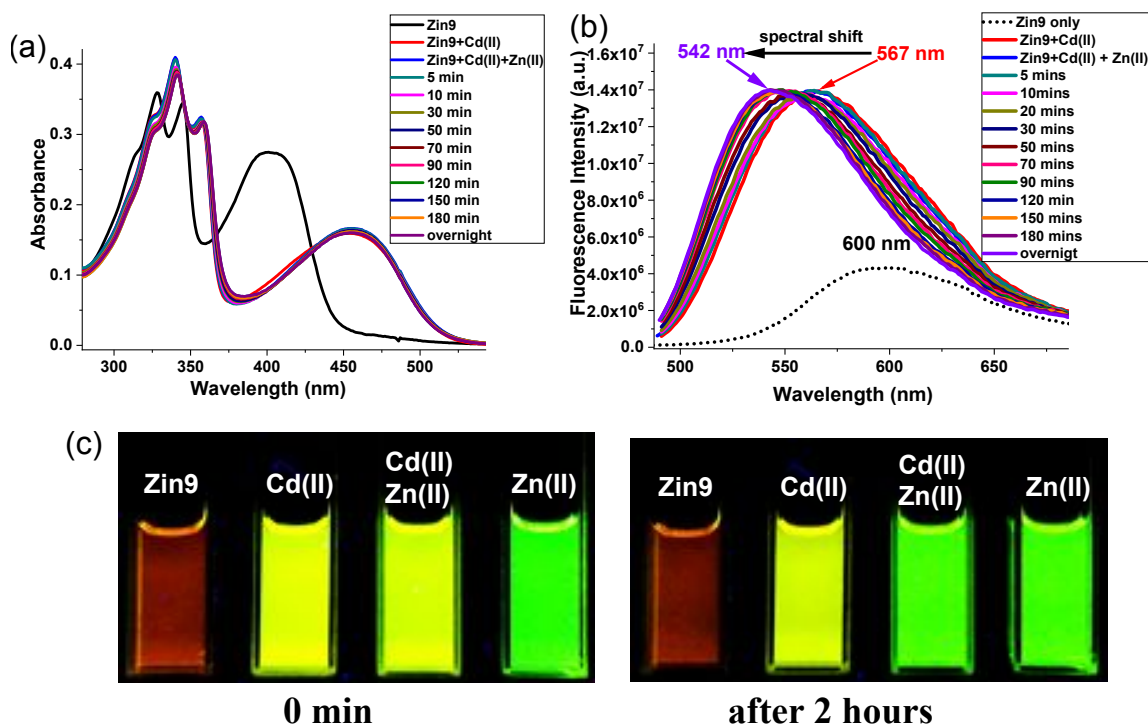


Fig. S23 UV-vis (a) and fluorescent spectra (b) change of **Zinhbo9** (8 μM) in HEPES buffer (pH = 7.4) containing 50% EtOH upon addition of 5.0 equivalent of Cd^{2+} first (well mixing), and then 5.0 equivalent of Zn^{2+} was added. The gradual spectral shift from 567 nm (yellow) to 542 nm (green) was observed in about 120 mins, which means the total replacement of Cd^{2+} by Zn^{2+} . (c) The images in the replacement experiment were captured under a 365 nm UV lamp.

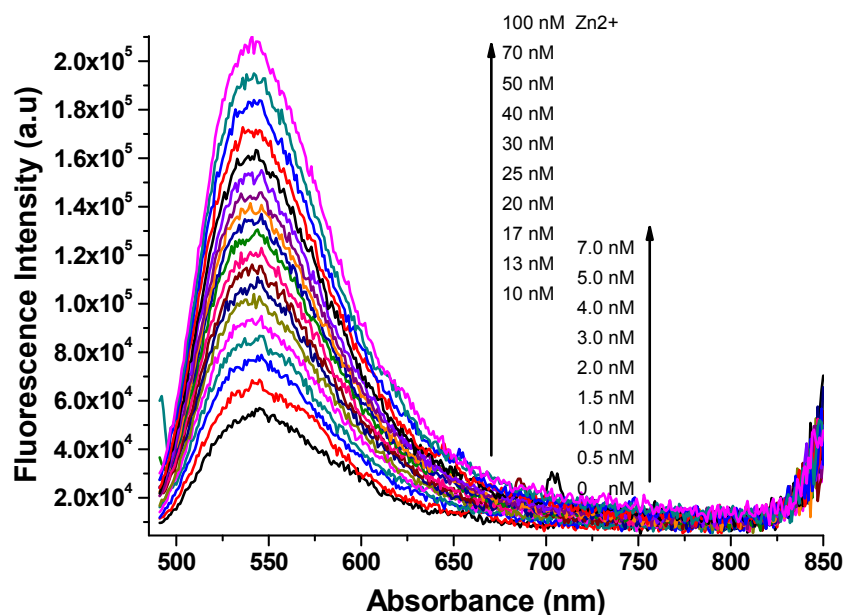


Fig. S24 Fluorescence intensity (monitored at 542 nm) of **Zinhbo-9** (500 nM) with different concentrations of Zn^{2+} ions in HEPES buffer (pH = 7.4) containing 50% EtOH excited at 470 nm.

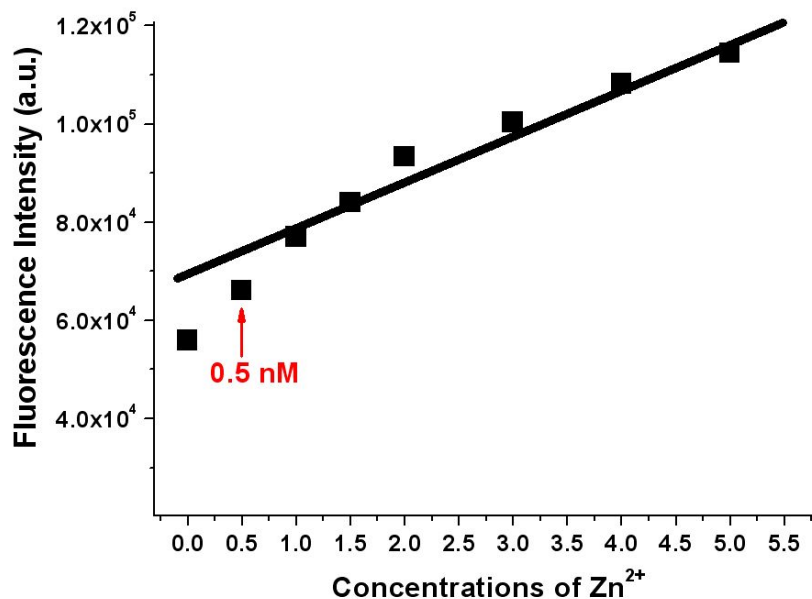


Fig. S25 Fluorescence plot of **Zinhbo-9** (500 nM) towards different concentrations of Zn^{2+} ions in HEPES buffer (pH = 7.4) containing 50% EtOH excited at 470 nm. The detection limit of Zinhbo9 towards Zn^{2+} was estimated at 0.5 nM.

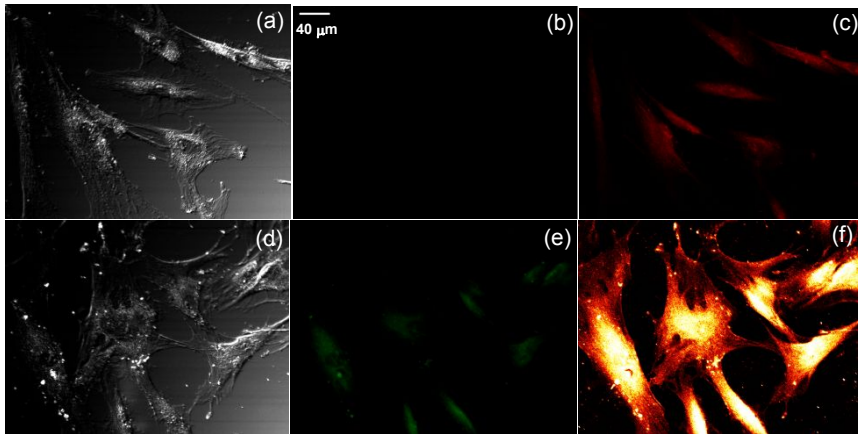


Figure S26. Confocal fluorescence images of Human mesenchymal stem cells (hMSCs) excited with a 488 nm laser. The cells were first incubated with 10 μM of Zn^{2+} for 30 mins and then further treated with 10 μM **Zinhbo-9** for another 60 minutes. The images were collected at bright field (a and d), green channel (b and e) and NIR channel (c and f: 700-800 nm). Top (control): the cells were incubated with **Zinhbo-9** for 60 mins at 37 $^{\circ}\text{C}$ in MSCBM (Lonza) medium; Bottom: the cells were first treated with Zn^{2+} (10 μM) for 30 mins and further exposed to **Zinhbo-9** (10 μM) for another 60 mins at 37 $^{\circ}\text{C}$ in MSCBM (Lonza) medium.

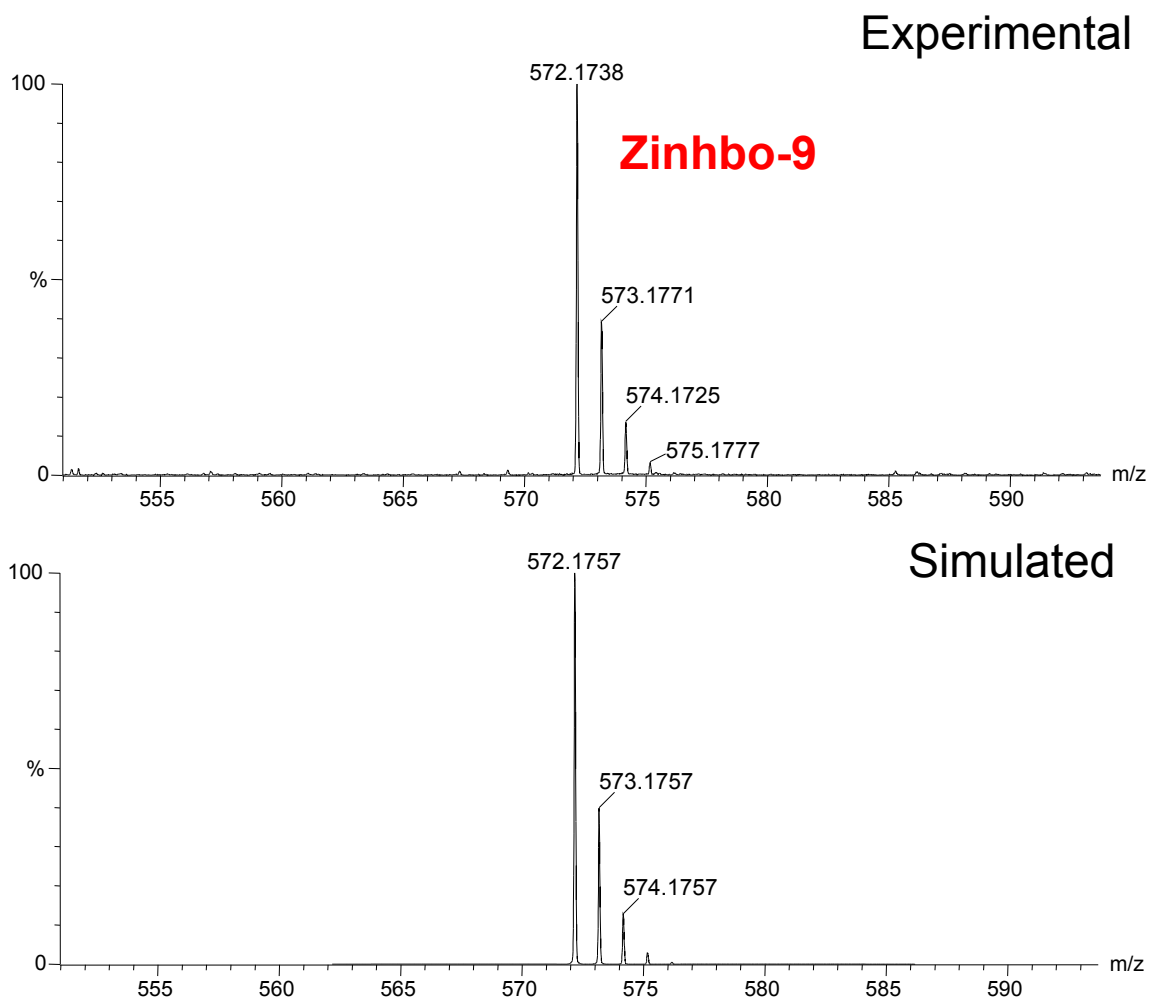


Fig. S27 ESI-Mass of **Zinhbo-9**: calcd for $C_{33}H_{26}N_5O_3Na$, $[M+H]^+$, 572.1757, found, 572.1738.

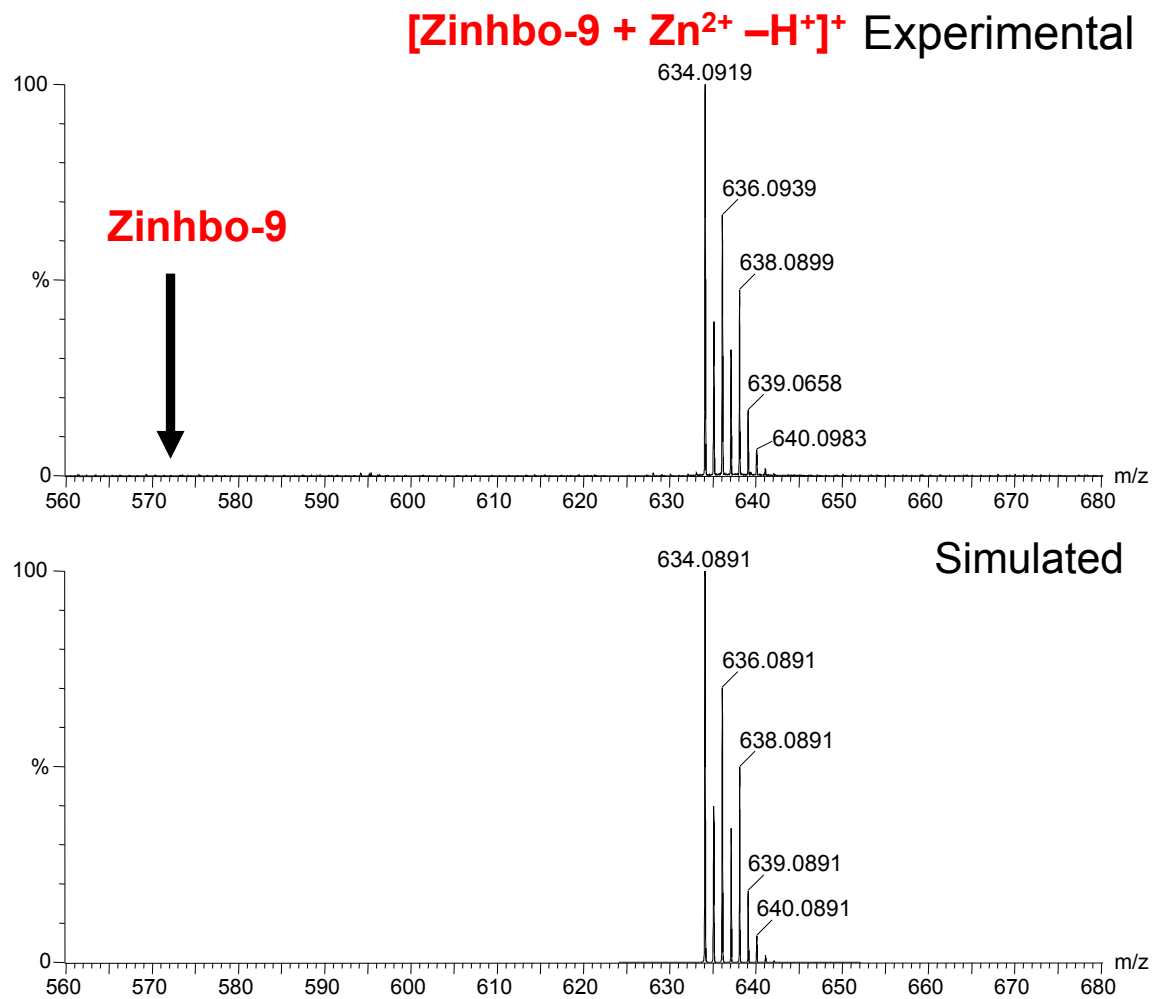
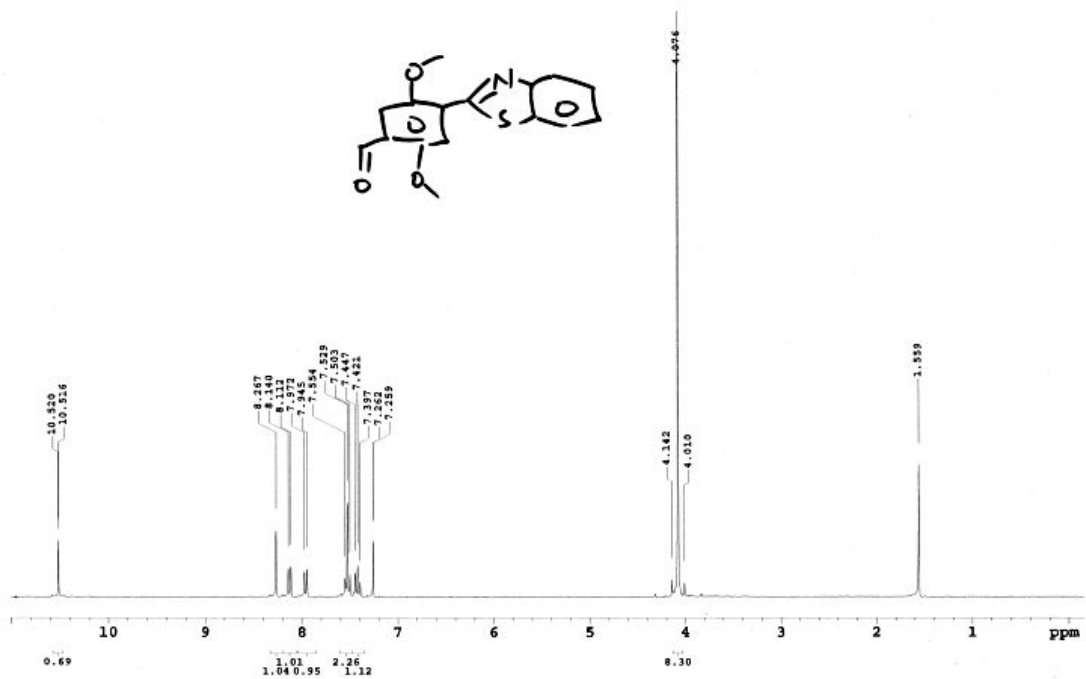


Fig. S28 ESI-Mass of **Zinhbo-9-Zn**: calcd for C₃₃H₂₄N₅O₃Zn, [M+Zn²⁺-H⁺]⁺, 634.0891, found, 634.0919.

Disnaphyl_2_Me_6_4_13_300
 Sample: ThioCHO
 Sample ID: s 20130718_02
 File: home/jw140/ThioCHO.fid
 Pulse Sequence: s2pul



Std Carbon experiment
 Sample: ThioCHO
 File: home/jw140/ThioCHO-C.fid
 Pulse Sequence: s2pul

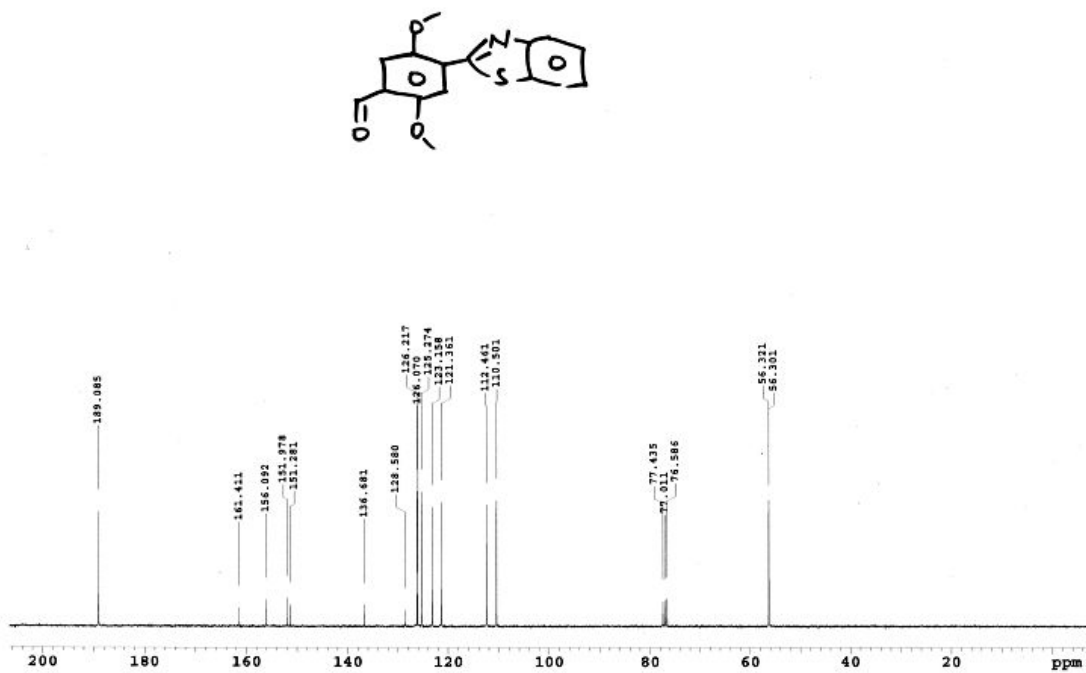
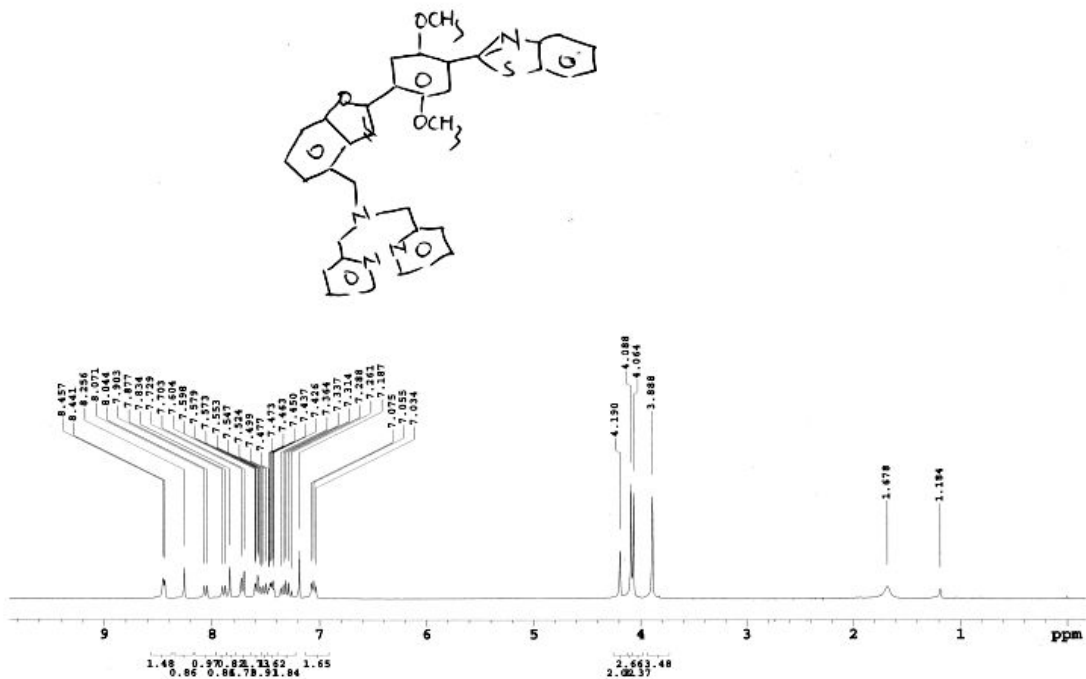


Fig. 29. ¹H NMR (top) and ¹³C NMR (bottom) spectra of **2** in CDCl₃.

Std Proton parameters
 Sample: wf193
 File: home/jwl40/wf193H.fid
 Pulse Sequence: s2pul



Std Carbon experiment
 Sample: wf193C
 File: home/jwl40/wf193C.fid
 Pulse Sequence: s2pul

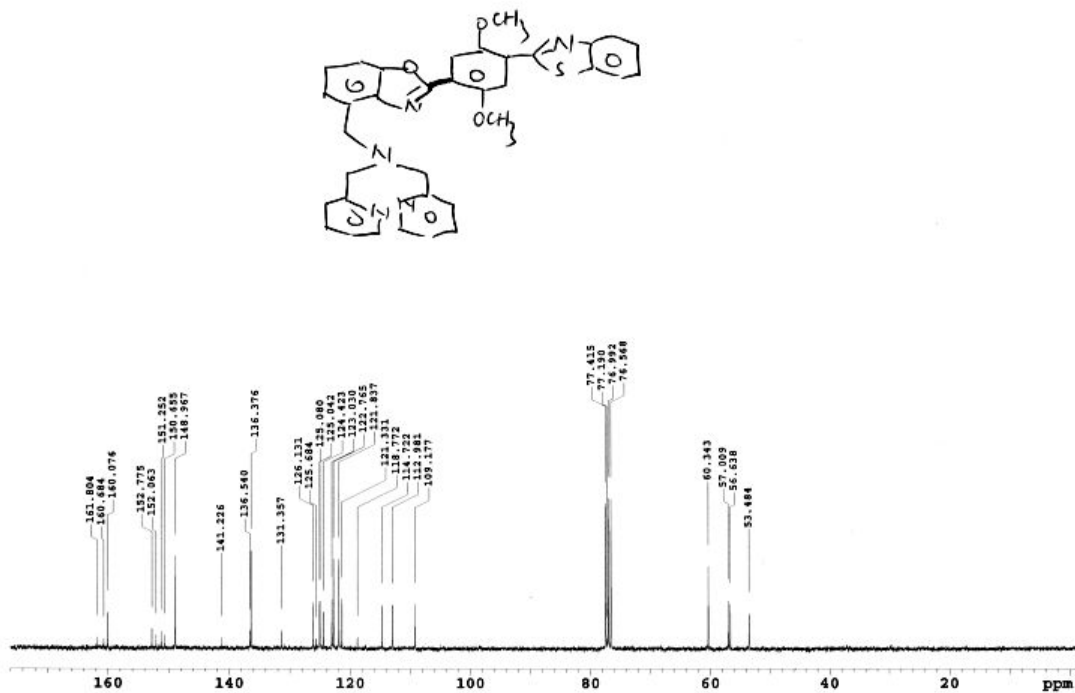
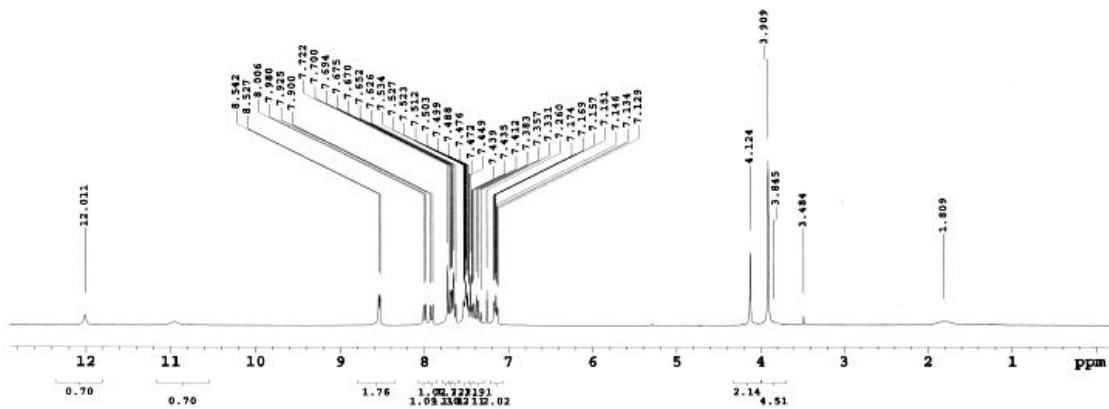
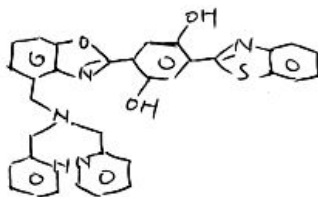


Fig. 30. ¹H NMR (top) and ¹³C NMR (bottom) spectra in CDCl₃.

Sample: wf199H
 Sample ID: s 20120911 01
 File: home/jw140/wf199H.fid
 Pulse Sequence: s2pul



Std Proton parameters
 Sample: wf199C
 Sample ID: s 20120911 02
 File: home/jw140/wf199C.fid
 Pulse Sequence: s2pul

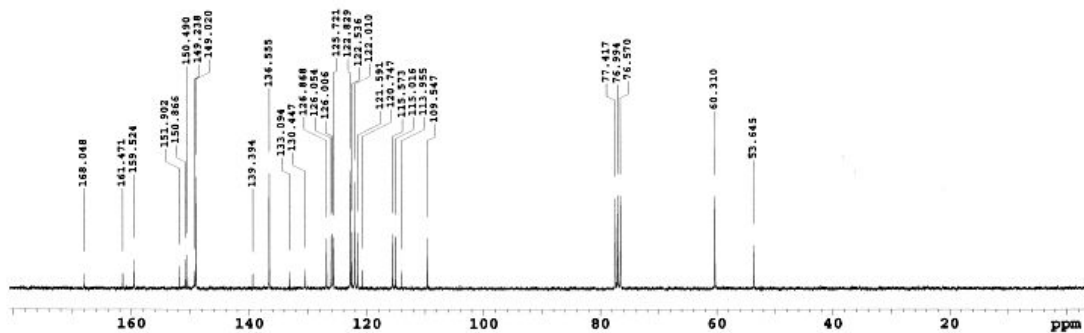
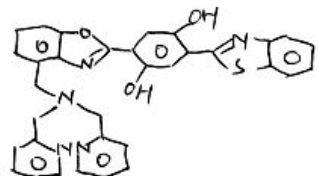


Fig. 31. ¹H NMR (top) and ¹³C NMR (bottom) spectra of **Zinhbo-9** in CDCl₃.